Microstructural investigation supporting an abrupt stress induced transformation in amorphous carbon films

D. W. M. Lau,[1,a)] J. G. Partridge,[1] M. B. Taylor,[1] D. G. McCulloch,[1] J. Wasyluk,[2] T. S. Perova,[2] and D. R. McKenzie[3]

[1]*Applied Physics, School of Applied Sciences, RMIT University, GPO Box 2476V Melbourne 3001, Australia*

[2]*Department of Electronic and Electrical Engineering, University of Dublin, Trinity College, Dublin 2, Ireland*

[3]*School of Physics, University of Sydney, New South Wales 2006, Australia*

(Received 15 August 2008; accepted 20 December 2008; published online 16 April 2009)

The intrinsic stress of carbon thin films deposited by filtered cathodic arc was investigated as a function of ion energy and Ar background gas pressure. The microstructure of the films was analyzed using transmission electron microscopy, electron energy loss spectroscopy, and Raman spectroscopy. The stress at given substrate bias was reduced by the presence of an Ar background gas and by the presence of a Cu underlayer deposited onto the substrate prior to deposition. Auger electron spectroscopy depth profiles showed no evidence of Ar incorporation into the films. A sharp transition from a sp^2 to sp^3 rich phase was found to occur at a stress of 6.5 ± 1.5 GPa, independent of the deposition conditions. The structural transition at this value of stress is consistent with available data taken from the literature and also with the expected value of biaxial stress at the phase boundary between graphite and diamond at room temperature. The microstructure of films with stress in the transition region near 6.5 GPa was consistent with a mixture of sp^2 and sp^3 rich structures. © *2009 American Institute of Physics*. [DOI: 10.1063/1.3075867]

I. INTRODUCTION

Amorphous carbon (*a*-C) thin films deposited using energetic condensation methods exhibit a wide variety of properties depending on the fabrication conditions.[1–4] At low energies (10 eV or less), films that have a majority of atoms in graphitelike (sp^2) bonding configurations are produced. With increasing energy, the material enters a new structural form [known as tetrahedral *a*-C or *ta*-C (Ref. 5)] with a majority of atoms in the diamondlike (sp^3) configuration. Films formed with energies higher than a few hundred eV have a low sp^3 fraction. In a recent paper,[6] we presented experimental evidence for a sharp boundary between the two distinct forms of amorphous carbon, the sp^3 rich phase and the sp^2 rich phase, when stress is used as the independent variable. The role of stress in the formation of *ta*-C has been debated in the literature, with some authors preferring a model in which the local processes occurring in the vicinity of an ion impact create conditions that locally form the high density tetrahedral phase.[7,8] Other authors prefer a model in which the tetrahedral phase is created because it is a stable phase under the prevailing high stress conditions created by the ion impacts[5,9] While it is difficult to make predictions from the two models that can distinguish between them, the existence of a sharp stress transition does not arise naturally from the first model.[8]

The existence of a sharp transition between the two phases in the *a*-C system suggests that the forms with intermediate sp^3 content are not stable. It is possible, however, to synthesize films that apparently have intermediate sp^3 fractions. Examination of the microstructure will help understand how the phase transition occurs in an amorphous system. In a crystalline system, a phase transition usually occurs by progression of a phase boundary between two distinct crystalline forms. The question arises as to whether intermediate *a*-C structures exist in the amorphous state or whether the material in the transition region consists of a mixture of two distinct amorphous structures.

By synthesizing films under a range of different conditions, the uniqueness of the value of the transition stress has been tested. We employed Ar background pressure to modify the ion energy distribution in a filtered cathodic vacuum arc (FCVA) deposition system. Although the FCVA is capable of operating in a vacuum, an inert background gas such as Ar is often used to stabilize the plasma.[10,11] However, the effect of background gas on the stress and microstructure of carbon films has only been investigated with fixed average ion energy.[11] This study includes experiments performed with a range of average ion energies between 9 and 820 eV. In addition, a Cu underlayer between the substrate and film was added with the intention of modifying the stress incorporated in the film under the impacts of a given ion energy. Electron diffraction, electron energy loss spectroscopy (EELS), and Raman spectroscopy are used to provide details on the microstructure of the films. Auger electron spectroscopy (AES) is used to determine whether any Ar is trapped in the films. We compare our results with available experimental data that relate the observed stress in *a*-C films to their sp^3 content.

[a)]Electronic mail: desmond.lau@rmit.edu.au.

 © 2009 American Institute of Physics

Downloaded 20 Apr 2009 to 134.226.86.54. Redistribution subject to AIP license or copyright; see http://jap.aip.org/jap/copyright.jsp

TABLE I. The operating parameters of the cathodic arc deposition system used to produce the three sets of samples. E_0 is the plasma potential measured using a Langmuir probe.

Deposition parameter	Series 1	Series 2	Series 3
Ar (ml/min)	0	7	15
Deposition Pressure (Torr)	6×10^{-6}	2×10^{-4}	6×10^{-6}
E_0 (eV)	20	13	9
Deposition rate at 75 V (nm/min)	0.4	0.2	0.06

II. EXPERIMENTAL METHODS

Carbon thin films were deposited onto silicon wafers using a dual bend filtered cathodic arc deposition system operating with a 99.9% pure graphite target, an arc current of 56 A, and a base pressure of better than 10^{-5} Torr. Three different flow rates of Ar were used with the deposition parameters provided in Table I. Silicon (100) substrates were cleaned prior to deposition in an ultrasonic bath, with acetone, ethanol, and distilled water before being air dried. The substrate holder was connected to a regulated dc power supply, allowing films to be deposited over a range of bias voltages from −25 to −1000 V. The average energy of the depositing species was calculated from the applied substrate bias by adding the plasma potential measured using a Langmuir probe for each of the Ar flow rates of Table I. The stress was determined from substrate curvature using Stoney's equation[12] and the film thickness was determined by step height measurements obtained using a Tencor P-16 profilometer. To obtain accurate stress values, two curvature measurements were performed in orthogonal directions on each substrate both before and after deposition. The thickness of the deposited films ranged from 10 to 85 nm. Films were also prepared on Cu underlayers of approximate thickness of 2 nm, which were sputter deposited onto the substrates prior to deposition.

The microstructure of the films was investigated using a JEOL 2010 transmission electron microscope (TEM) operating at 200 kV. Plan view samples were prepared by acid (48% concentrated HF) etching of the silicon wafers. A selection of samples was also prepared in cross section by a combination of mechanical tripod polishing and Ar ion beam thinning. EELS analysis was performed using a Gatan Imaging Filter (GIF2000). An EELS spectrum was collected in the low loss region in order to determine the plasmon peak position. The peak position was then used to calculate the film density assuming carbon has four valence electrons, each with an effective mass of $0.87m_e$, taking part in plasmon oscillations.[13,14] EELS spectra were also collected in the region of the carbon K-shell ionization edge so that the fraction of sp^2 bonded carbon atoms could be estimated.[15] Energy filtered electron diffraction patterns were collected using the GIF2000 with procedures outlined elsewhere.[16] A VG310F scanning auger nanoprobe was utilized to measure the Ar content of the films by performing elemental depth profiles in which Xe was used as the sputtering gas.

The micro-Raman scattering measurements were carried out at room temperature in the backscattering geometry using RENISHAW 1000 micro-Raman system equipped with a

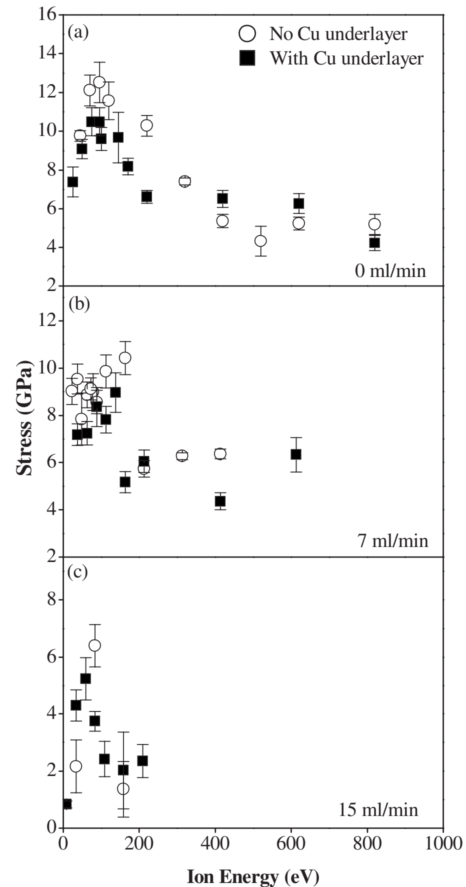

FIG. 1. The intrinsic stress measured as a function of ion energy for carbon thin films deposited with various Ar flow rates of (a) 0, (b) 7, and (c) 15 ml/min with and without a Cu underlayer.

charge coupled device camera and a Leica microscope. A grating with 1800 lines/mm was used for all measurements, providing a spectral resolution of ~1 cm^{-1}. An Ar^+ laser at 457 nm with power of 10 mV was used as the excitation source. The Raman spectra were taken in two modes: the extended mode with 30 s exposure time and 5 accumulations in the range of 400 to 4000 cm^{-1} and the static mode with 10 accumulations and 30 s registration time in the range of 810 to 1950 cm^{-1}. The laser spot was focused on the sample surface using a 50× objective.

III. RESULTS

A. Intrinsic stress

Figure 1 shows the effect of increasing Ar flow rates on the intrinsic stress of carbon films deposited at a range of ion energies. Figure 1(a) shows that films prepared in the absence of Ar have the typical stress versus ion energy curve previously described for FCVA deposited films.[5,17] The peak in the stress curve at 12.5 GPa was found to occur at an average ion energy of 95 eV. The effect of a Cu underlayer is to reduce the stress induced in the film by ions with energies up to approximately 200 eV. Adding 7 ml/min of Ar [results shown in Fig. 1(b)] extends the stress peak to lower energies and reduces the maximum stress to approximately 10 GPa. Introducing Ar at this flow rate during a deposition with average ion energy of 95 eV also halved the deposition rate

Downloaded 20 Apr 2009 to 134.226.86.54. Redistribution subject to AIP license or copyright; see http://jap.aip.org/jap/copyright.jsp

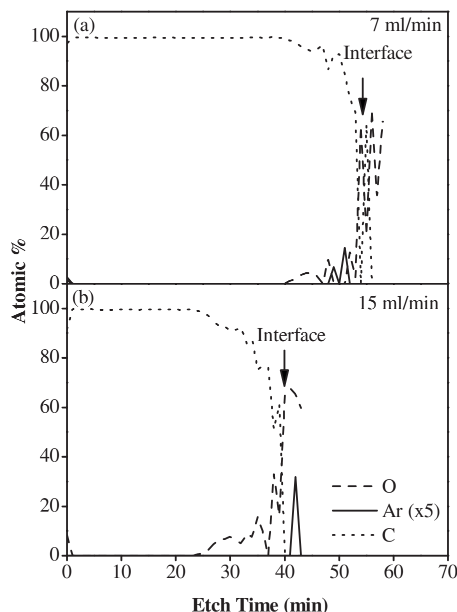

FIG. 2. AES depth profiles for films grown using Ar flow rates of (a) 7 ml/min at 88 eV and (b) 15 ml/min at 159 eV. The arrow indicates the film/substrate interface.

(see Table I). There is no net film growth at energies above 600 eV. Increasing the Ar flow rate to 15 ml/min reduces the peak stress to approximately 6 GPa, which further reduces the deposition rate and prevents film growth for energies above 200 eV. The reduction in deposition rate may be the result of increased collisions between the background Ar and the incoming C ions and increased sputtering by Ar ions.

B. Compositional depth profiles

Figure 2 shows AES depth profiles that confirm no Ar was incorporated into the films at either 7 or 15 ml/min flow rate. Ar was detected at the film/substrate interface (indicated by an arrow), possibly as a result of ion implantation during the initial stages of film growth.

C. Cross sectional TEM

Figure 3 shows a cross sectional TEM image of a film prepared using an average ion energy of 60 eV, with 15 ml/min of Ar background gas and with a 2 nm thick Cu underlayer. There is no evidence of voids or bubbles that could be associated with Ar incorporation into the films. Note that the silicon substrate has an approximately 6 nm thick surface oxide.

D. Density and sp^2 fraction

Figure 4(a) shows the relationship between stress and density calculated from the plasmon peak position for samples prepared with and without a Cu underlayer using a range of Ar flow rates. A point is included for an *a*-C film of low stress prepared using sputtering. All the films fall on the same curve with a transition from a low to a high density phase occurring at a stress of 6.5 ± 1.5 GPa. We term this region of stress the "transition region." For the same samples, the relation between density and sp^2 fraction is given in Fig. 4(b) and shows a linear relation.

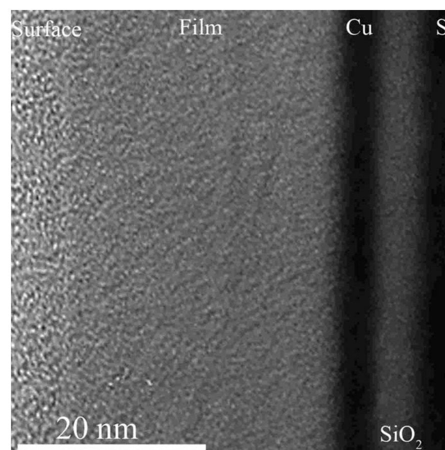

FIG. 3. Cross-sectional TEM image of an *a*-C film deposited onto a Cu underlayer with an average ion energy of 60 eV and an Ar flow rate of 15 ml/min. The Cu underlayer and Si substrate as dark regions.

E. Energy filtered electron diffraction

Figure 5 shows radially averaged energy filtered diffraction patterns for selected carbon films. Also shown is the diffraction pattern for glassy carbon, which is a fully sp^2 bonded structure with well formed graphitic sheets. The diffraction pattern for the film prepared at low energy and at a relatively low stress of approximately 5 GPa shows diffuse rings typical of a sp^2 rich amorphous network. This diffraction pattern also shows strong scattering at small angles indicative of the presence of mesoscale inhomogeneities. The film prepared using 84 eV at a stress of 6.9 GPa develops a graphitic {002} peak as a shoulder. This film is in the transition region and shows features characteristic of both partially ordered graphite and an amorphous carbon. Films in the transition region prepared at energies above 300 eV (as shown in

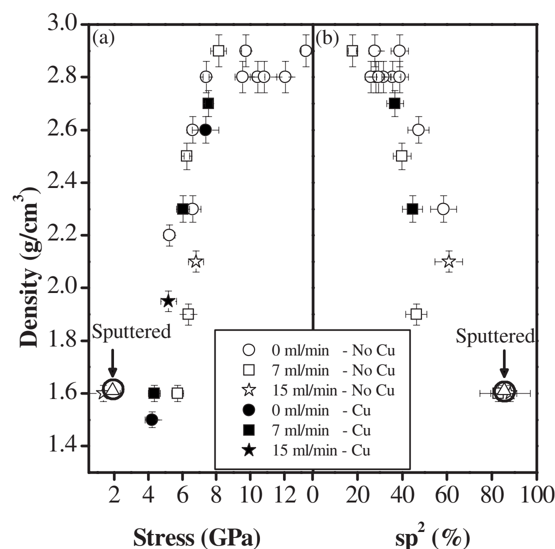

FIG. 4. The density of carbon films as a function of (a) stress and (b) sp^2 content. The films were deposited under the indicated flow rates of Ar in the presence or absence of a Cu underlayer.

Downloaded 20 Apr 2009 to 134.226.86.54. Redistribution subject to AIP license or copyright; see http://jap.aip.org/jap/copyright.jsp

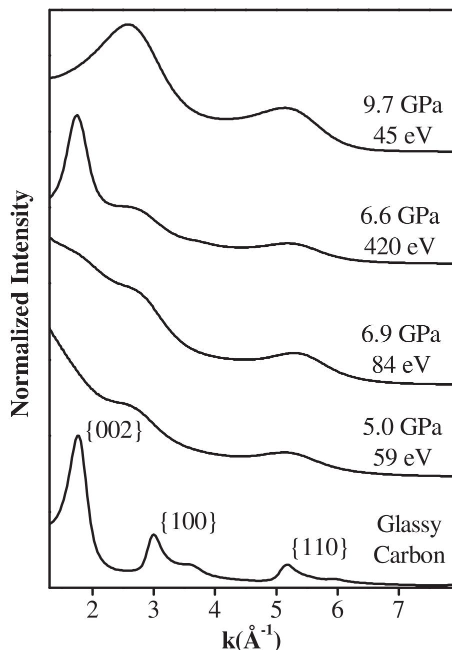

FIG. 5. Radially averaged energy filtered diffraction patterns for a range of carbon films prepared at the energy and stress conditions indicated. Also shown for comparison is the diffraction pattern for glassy carbon, which has been indexed to graphite.

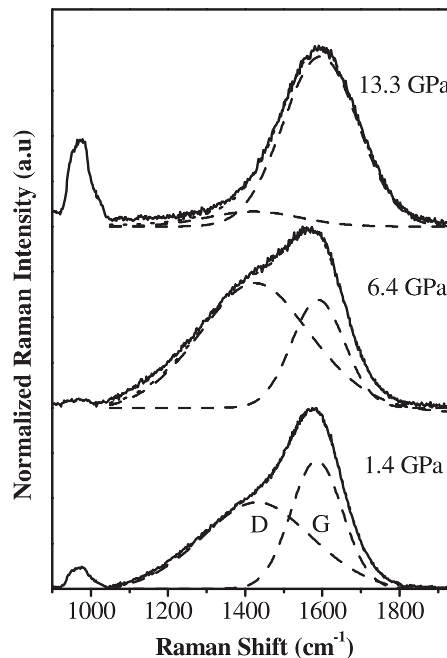

FIG. 6. Raman spectra of selected *a*-C films with increasing stress. Featured include the second order Si feature at 960 cm^{-1} together with the *D*-peak ($\sim$1400 cm^{-1}) and *G*-peak ($\sim$1580 cm^{-1}) fitted to each spectrum using mixtures of Gaussian and Lorentzian functions (shown as dashed curves).

Fig. 5 for the case of 6.6 GPa and 420 eV) show a well formed {002} peak indicative of well ordered graphitic planes. As described elsewhere,[6] films prepared under these conditions develop preferred orientation and contain graphitic planes aligned normal to the sample surface. The diffraction pattern for the film grown with a high stress of 9.7 GPa shown in Fig. 5 is typical of *ta*-C (Ref. 18) and exhibits very low intensity near the undiffracted beam, indicating a dense homogeneous network.

F. Raman spectroscopy

Raman spectra were obtained for *a*-C films prepared at a range of stress values and several examples are shown in Fig. 6. The following Raman features were observed: *a*-Si band at about 960 cm^{-1} due to the second order phonon scattering from the silicon substrate, a carbon *D* (disorder) band around at 1400 cm^{-1}, and a carbon *G* (graphitic) band at about 1580 cm^{-1}. The *G*- and *D*-peaks are due to sp^2 sites only.[19] The *G*-peak is due to the bond stretching of all pairs of sp^2 atoms in both rings and chains and the *D*-peak is due to the breathing modes of sp^2 rings.[19] The intensity of the second order Si peak depends on the thickness of the film and its absorption coefficient at the corresponding wavelength.

The spectra were fitted with two carbon peaks using mixtures of Gaussian and Lorentzian functions.[20,21] As can be seen from Fig. 6 the experimental spectra are fitted very well using this approach. Figure 7(a) shows the *G* and *D* integrated intensity ratio I_D/I_G as a function of the sp^2 content in the *a*-C films. I_D/I_G increases with increased sp^2 content. This indicates that sp^2 sites are beginning to organize into small graphitic clusters.[22] Figure 7(b) shows the Raman shift of the *G*-peak as a function of sp^2 content. The *G*-peak position decreases nonlinearly with increasing sp^2 content

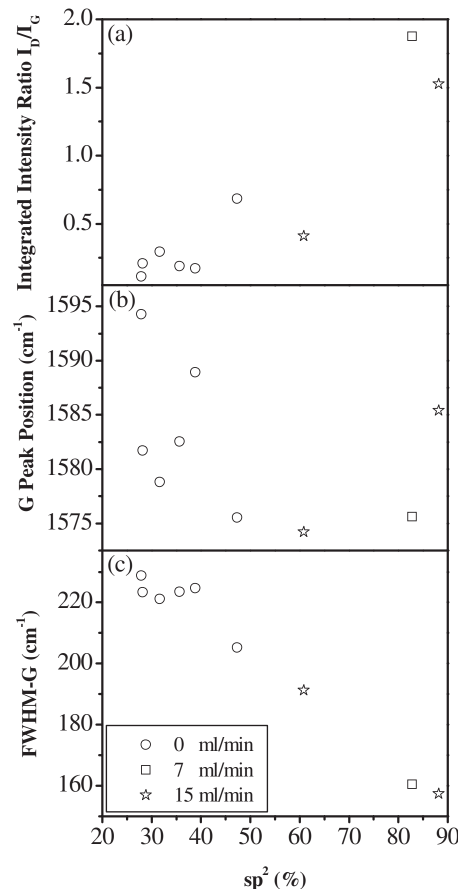

FIG. 7. Peak position analysis of Raman spectra as a function of sp^2 content, showing (a) integrated intensity ratio (I_D/I_G) of the *D*- and *G*-peaks (b) *G*-peak position and (c) the *G*-peak FWHM. The films were deposited under the indicated flow rates of Ar.

Downloaded 20 Apr 2009 to 134.226.86.54. Redistribution subject to AIP license or copyright; see http://jap.aip.org/jap/copyright.jsp

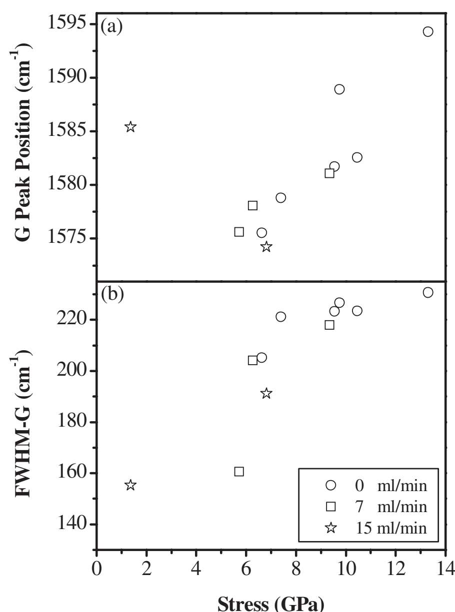

FIG. 8. (a) The *G*-peak position and (b) *G*-peak FWHM in the Raman spectra of films deposited under the indicated flow rates of Ar.

and asymptotes toward 1575 cm^{-1} as the sp^2 fraction increases. This decrease in *G*-peak position as the sp^2 fraction increases has been observed previously[23] and was attributed to a change in the arrangement of sp^2 sites from small chains or dimers to rings. Figure 7(c) shows that there is a linear relationship between the *G*-peak full width at half maximum (FWHM) and sp^2 content. This result is consistent with increasing graphitic ordering within the films at higher sp^2 contents, resulting in a narrowing of the *G*-peak.

Figure 8(a) shows the *G*-peak position as a function of stress. A linear relationship is observed for stresses above 4 GPa. As the stress increases, the *G*-peak shifts to higher wave numbers. This is expected on the basis of an increase in lattice vibration frequencies when the amorphous network is compressed.[24] The relationship between stress and *G*-peak FWHM is shown in Fig. 8(b). A transition is observed at ~6.5 GPa between high sp^2 content films and low sp^2 content films. This observation confirms that a microstructural transition occurs at this value of stress, as was evident from the density measurements in Fig. 4(a).

IV. DISCUSSION

In the absence of Ar, the intrinsic stress of the carbon films increases with ion energy up to a maximum of ~12 GPa at 95 eV before decreasing at higher energies. This behavior has been observed previously[5,17] and has been interpreted as a competition between stress generation (when ions impact with energies 10–100 eV) and stress relief processes (when ions impact at ion energies >100 eV).[25,26] Measurements of the energy distribution of C ions ejected from a cathodic arc source operating in a vacuum show a relatively narrow distribution around the mean energy.[27] When Ar is introduced as a background gas, two main effects occur. The first is an asymmetric broadening to lower energies of the energy distribution of the incident C ions as a result of collisions with Ar. As a result, fewer ions have the optimal energy for stress generation and the stress maximum at 95 eV is lowered to approximately 10 GPa in the case of 7 ml/min of Ar flow rate. These results are consistent with previous findings,[11] in which a lowering of stress was observed in the presence of Ar for samples prepared at earth potential.

The second effect of introducing Ar into the deposition process is bombardment of the substrate by Ar ions. At lower energies, these ions can generate compressive stress, a process that is exploited in ion assisted deposition.[28] The result is increased stress in films grown with biases below 75 V. As the bias is increased, the sputter yield increases and no net film growth occurs. For the higher Ar flow rate of 15 ml/min, the mean free path is very short so that the average C ion energy is low. In this case, the stress generation mechanism is likely to be dominated by Ar bombardment. The higher mass of the Ar ions relative to C ions results in a stress maximum at a lower bias value.

The Raman analysis confirms results from the TEM studies, which show a sharp transition from a low density *a*-C to a high density *ta*-C structural phase at a stress of approximately 6.5 GPa. The value of the transition stress is not affected by Ar flow rate or the presence or absence of a Cu underlayer. This proves that the transition is induced at a fixed value of stress and not by the conditions that gives rise to the stress. Within the transition region, diffraction analysis shows evidence for a material that contains more than one type of microstructure. Referring to the sample prepared at 84 eV (Fig. 5) in the transition region, the peak at $k=1.77$ Å^{-1} indicates the presence of material with sp^2 bonding and the peak at $k=2.8$ Å^{-1} in the same diffraction pattern indicates the presence of *ta*-C. An almost identical diffraction pattern has been observed previously in ion implanted *ta*-C in which the microstructure was found to be a mixture of *ta*-C and sp^2-rich *a*-C clusters created by ion beam damage.[18] It is conceivable that this type of microstructure may be present in the films in the transition region of this study. Films prepared within the transition region at high energies (see the sample prepared at 420 eV in Fig. 4) also show evidence of more than one type of microstructure. However, in this case, the sp^2 rich phase contains oriented graphene sheets, as described previously,[6] which result in a sharp {002} graphitic reflection.

Figure 9 shows the sp^3 fraction (measured using EELS) as a function of stress for our films compared with values obtained for pure carbon taken from the literature. We only considered films that have been synthesized at room temperature without intentional doping since the presence of dopant atoms[29,30] is known to influence bonding and hence is likely to modify the transition stress. The scatter in the data at high sp^3 content is due to difficulty in measuring the decreasing levels of π-bonding using EELS.[31] The majority of the data are consistent with the proposition that there is a transition region between 5 and 8 GPa (shown as a shaded band) separating low and high density forms of *a*-C. The outlying points (circled in Fig. 9) at low stress and high sp^3 content may be the result of substrate heating during deposition, giving rise to a reduction in stress by annealing.[32] The value of 6.5 GPa is close to the biaxial stress expected to

Downloaded 20 Apr 2009 to 134.226.86.54. Redistribution subject to AIP license or copyright; see http://jap.aip.org/jap/copyright.jsp

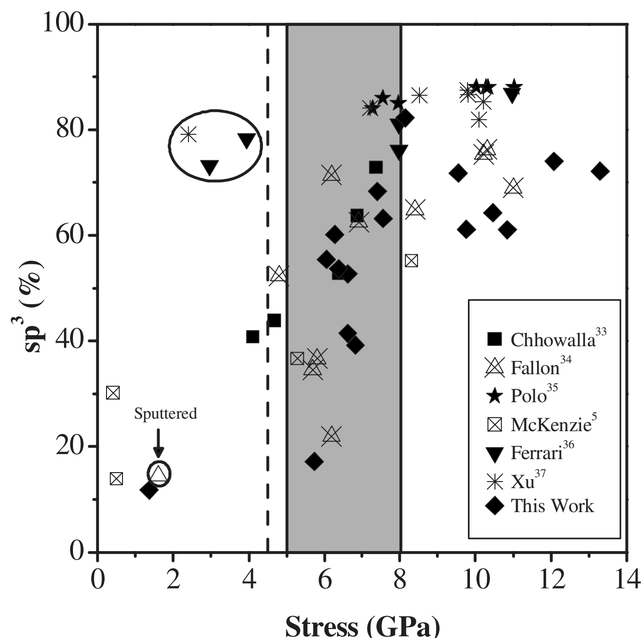

FIG. 9. The sp^3 fraction (measured by EELS) as a function of stress for of *a*-C films prepared at room temperature and measured by different groups (Refs. 5 and 33–37). The majority of points show the differentiation between the phases of low and high sp^3 fraction, separated by a transition region at 6.5 ± 1.5 GPa shown as the shaded band. The outlying points (circled) at low stress and high sp^3 content may be the result of substrate heating during deposition, which reduces stress by annealing. The vertical dotted line indicates the biaxial stress expected to mark the boundary between graphite and diamond at room temperature (Ref. 5).

mark the boundary between graphite and diamond at room temperature, which has been calculated to be 4.5 GPa.[5]

V. CONCLUSION

We have shown that the introduction of Ar as a background gas during deposition of *a*-C films reduces the intrinsic stress at a given substrate bias. The presence of a Cu underlayer also reduced stress. The added Ar reduced the kinetic energy of incident carbon ions by ion-atom collisions and increased sputtering. A sharp transition between sp^2-rich and sp^3-rich forms of *a*-C was observed at a stress of 6.5 GPa, independent of the deposition conditions. This observation provides strong evidence that stress is the driving force behind the formation of the sp^3-rich *ta*-C phase. A compilation of available data from the literature supports the proposition of a stress induced transition at 6.5 GPa. Diffraction analysis of the microstructure of films with stresses in the transition region is consistent with the presence of two phases rather than a single homogeneous phase with an intermediate sp^3 fraction.

ACKNOWLEDGMENTS

The authors would like to thank J. L. Peng for assistance in preparing the TEM samples. The authors also acknowledge the financial support provided by the Australian Research Council (ARC).

[1] A. Ilie, A. C. Ferrari, T. Yagi, S. E. Rodil, J. Robertson, E. Barborini, and P. Milani, J. Appl. Phys. **90**, 2024 (2001).
[2] E. G. Gerstner and D. R. McKenzie, Diamond Relat. Mater. **7**, 1172 (1998).
[3] J. Robertson, Thin Solid Films **383**, 81 (2001).
[4] D. R. McKenzie, R. N. Tarrant, M. M. M. Bilek, T. Ha, J. Zou, W. E. McBride, D. J. H. Cockayne, N. Fujisawa, M. V. Swain, and N. L. James, Diamond Relat. Mater. **12**, 178 (2003).
[5] D. R. McKenzie, D. Muller, and B. A. Pailthorpe, Phys. Rev. Lett. **67**, 773 (1991).
[6] D. W. M. Lau, D. G. McCulloch, M. B. Taylor, J. G. Partridge, D. R. McKenzie, N. A. Marks, E. H. T. Teo, and B. K. Tay, Phys. Rev. Lett. **100**, 176101 (2008).
[7] Y. Lifshitz, G. D. Lempert, and E. Grossman, Phys. Rev. Lett. **72**, 2753 (1994).
[8] J. Robertson, Diamond Relat. Mater. **3**, 361 (1994).
[9] D. G. McCulloch, D. R. McKenzie, and C. M. Goringe, Phys. Rev. B **61**, 2349 (2000).
[10] S. Anders and B. Juttner, IEEE Trans. Plasma Sci. **19**, 705 (1991).
[11] T.-Y. Kim, C. S. Lee, Y. J. Lee, K.-R. Lee, K.-H. Chae, and K. H. Oh, J. Appl. Phys. **101**, 023504 (2007).
[12] G. G. Stoney, Proc. R. Soc. London, Ser. A **82**, 172 (1909).
[13] L. Calliari, S. Fanchenko, and M. Filippi, Diamond Relat. Mater. **16**, 1316 (2007).
[14] R. F. Egerton, *Electron Energy-Loss Spectroscopy in the Electron Microscope*, 2nd ed. (Plenum, New York, 1996).
[15] S. D. Berger, D. R. McKenzie, and P. J. Martin, Philos. Mag. Lett. **57**, 285 (1988).
[16] T. C. Petersen, W. McBride, D. G. McCulloch, I. K. Snook, and I. Yarovsky, Ultramicroscopy **103**, 275 (2005).
[17] B. K. Tay, X. Shi, L. K. Cheah, and D. I. Flynn, Thin Solid Films **308–309**, 199 (1997).
[18] D. G. McCulloch, E. G. Gerstner, D. R. McKenzie, S. Prawer, and R. Kalish, Phys. Rev. B **52**, 850 (1995).
[19] A. C. Ferrari and J. Robertson, Phys. Rev. B **64**, 075414 (2001).
[20] S. S. Roy, P. Papakonstantinou, R. McCann, G. Abbas, J. P. Quinn, and J. McLaughlin, Diamond Relat. Mater. **13**, 1459 (2004).
[21] F.-X. Liu, K.-L. Yao, and Z.-L. Liu, Diamond Relat. Mater. **16**, 1746 (2007).
[22] A. C. Ferrari, Diamond Relat. Mater. **11**, 1053 (2002).
[23] A. C. Ferrari and J. Robertson, Phys. Rev. B **61**, 14095 (2000).
[24] J.-K. Shin, C. S. Lee, K.-R. Lee, and K. Y. Eun, Appl. Phys. Lett. **78**, 631 (2001).
[25] C. A. Davis, Thin Solid Films **226**, 30 (1993).
[26] M. M. M. Bilek and D. R. McKenzie, Surf. Coat. Technol. **200**, 4345 (2006).
[27] E. Byon and A. Anders, J. Appl. Phys. **93**, 1899 (2003).
[28] L. K. Cheah, X. Shi, B. K. Tay, and E. Liu, Surf. Coat. Technol. **105**, 91 (1998).
[29] S. Bhattacharyya, M. Hietschold, and F. Richter, Diamond Relat. Mater. **9**, 544 (2000).
[30] M. Tan, J. Zhu, J. Han, X. Han, L. Niu, and W. Chen, Scr. Mater. **57**, 141 (2007).
[31] Y. Lifshitz, Diamond Relat. Mater. **12**, 130 (2003).
[32] M. Chhowalla, J. Robertson, C. W. Chen, S. R. P. Silva, C. A. Davis, G. A. J. Amaratunga, and W. I. Milne, J. Appl. Phys. **81**, 139 (1997).
[33] M. Chhowalla, Y. Yin, G. A. J. Amaratunga, D. R. McKenzie, and T. Frauenheim, Appl. Phys. Lett. **69**, 2344 (1996).
[34] P. J. Fallon, V. S. Veerasamy, C. A. Davis, J. Robertson, G. A. J. Amaratunga, W. I. Milne, and J. Koskinen, Phys. Rev. B **48**, 4777 (1993).
[35] M. C. Polo, J. L. Andujar, A. Hart, J. Robertson, and W. I. Milne, Diamond Relat. Mater. **9**, 663 (2000).
[36] A. C. Ferrari, S. E. Rodil, J. Robertson, and W. I. Milne, Diamond Relat. Mater. **11**, 994 (2002).
[37] S. Xu, B. K. Tay, H. S. Tan, L. Zhong, Y. Q. Tu, S. R. P. Silva, and W. I. Milne, J. Appl. Phys. **79**, 7234 (1996).

Downloaded 20 Apr 2009 to 134.226.86.54. Redistribution subject to AIP license or copyright; see http://jap.aip.org/jap/copyright.jsp